

# Effect of $\text{Pr}_6\text{O}_{11}$ Substitution on Structural and Dielectric Properties of $\text{BaZrTiO}_5$ Ceramic Materials

Osama A. Desouky<sup>\*1</sup>; K. E. Rady<sup>2</sup>

<sup>1</sup>Bilbis Higher Institute of Engineering (BHIE), Bilbis, Sharqia , Egypt

<sup>2</sup>Engineering Basic Sciences Department, Faculty of Engineering, Menoufia University, Shebin El-Kom, Egypt

\*Corresponding author mail: Osama\_Amin2015@ yahoo.com

**Abstract** — In the present work, we studied the effect of the substitution of BaO by  $\text{Pr}_6\text{O}_{11}$ , on the structure, dielectric and electrical properties of  $\text{BaTiZrO}_5$  ceramics. Samples of general formula  $(99.2-x) \text{BaO} \cdot x\text{Pr}_6\text{O}_{11} \cdot 0.5\text{TiO}_2 \cdot 0.3\text{ZrO}_2$  ( $x = 0.1, 0.2, 0.5$  and  $0.6$ ) named P<sub>1</sub>, P<sub>2</sub>, P<sub>3</sub> and P<sub>4</sub> respectively were prepared by conventional ceramic method. The structure of the prepared samples was studied using X-ray diffraction, water absorption % and SEM. Addition of  $\text{Pr}_6\text{O}_{11}$  minimized the presence of closed pores and thus led to improved densification. The crystallize size of the prepared samples was calculated and found in the range 22-26 nm. The effect of the substitution by  $\text{Pr}_6\text{O}_{11}$  on breakdown field, dielectric constant, ac resistivity was investigated. Finally, it was found that, the substitution BaO by  $\text{Pr}_6\text{O}_{11}$  improves the physical properties of  $\text{BaTiZrO}_5$  ceramics by increasing their break down field, ac resistivity and dielectric constant that makes these ceramics useful in the technological applications.

**Keywords:** *BaTiZrO<sub>5</sub> ceramics; water absorption; breakdown field SEM; dielectric constant; ac resistivity.*

## I. INTRODUCTION

$\text{BaTiO}_3$  ceramics is a ferroelectric material with a high dielectric constant and high insulation resistance. Therefore, it used in electric ceramic capacitors, thermistors, piezoelectric transducers and a variety of electro-optic devices [1, 2]. Barium titanate

( $\text{BaTiO}_3$ ) a perovskite structure, has been widely investigated because of its dielectric and ferroelectric properties [3, 4]. Ceramics materials based on  $\text{BaTiO}_3\text{-R}_2\text{O}_3$  system (R = rare earth, mostly Zr, Pr, La and Nd) are used for preparation passive electronic components.  $\text{BaTiO}_3$  slightly doped with rare earth oxides is semi-conductor and is used for manufacture of switching, heating and regulating devices. The increasing of amounts of rare earths oxides with  $\text{BaTiO}_3$  exhibits high electrical resistivity and is used in manufacturing high stable capacitors [5].

The electric properties of  $\text{BaTiO}_3\text{-R}_2\text{O}_3$  depend on the chemical composition, crystal structure, and grain size. To produce semiconductive ceramics, a small amount of rare metal oxide such as  $\text{ZrO}_2$ ,  $\text{Pr}_2\text{O}_3$  was added [6, 7].  $\text{ZrO}_2$  plays a critical role in maintaining the electrical properties of  $\text{BaTiO}_3$  ceramics. It was found that, the sintering temperature of  $\text{BaZrTiO}_3$  is always (1350 -1400°C), when  $\text{ZrO}_2$ , ZnO, CuO and  $\text{SiO}_2$  are added, the sintering temperature

decrease by 100-300°C and dielectric constant rising [8-10]. The (Ca, Zr) co-doped BaTiO<sub>3</sub> ceramics was earlier used in capacitor composition [11-13].

Praseodymium oxide is a rare earth metal oxide that has not been used for microelectronic applications so far. Based on thermo dynamical considerations it should be stable against silicon. Praseodymium oxide (PrO<sub>x</sub>) has different oxygen compositions, with x ranging from 1.5 to 2 due to the multiple oxidation states (+3 and +4) of Pr. Variations in oxygen vacancy ordering lead to different phases including two cubic phases for PrO<sub>2</sub> and manganese oxide (Mn<sub>2</sub>O<sub>3</sub>) structure for Pr<sub>2</sub>O<sub>3</sub>. In addition, praseodymium oxide exhibits negligible hysteresis and excellent reliability characteristics. The partial replacement of Ti<sup>4+</sup> by Sn<sup>4+</sup> produces the BaTi<sub>1-x</sub>Sn<sub>x</sub>O<sub>3</sub>, solid solution that shows diffuse phase-transition behavior and Curie temperature (T<sub>C</sub>) decreases with the Sn<sup>4+</sup> incorporation [14-16]. Recently, the effect of rare earth metal ions on the structural and electrical properties of BaTiO<sub>3</sub> has been studied by many authors [17-19].

In the present work the effect of the substitution by a small amount of rare earth metal oxide such as Pr<sub>6</sub>O<sub>11</sub> on the structure, electrical and dielectric properties of BaZrTiO<sub>5</sub> ceramics is investigated.

## II. EXPERIMENTAL

Samples of general formula (99.2-x) BaO-xPr<sub>6</sub>O<sub>11</sub>-0.5TiO<sub>2</sub>-0.3ZrO<sub>2</sub> (x = 0.1, 0.2, 0.5 and 0.6) named P<sub>1</sub>, P<sub>2</sub>, P<sub>3</sub> and P<sub>4</sub> respectively were prepared by conventional ceramic method using high-purity oxide powders BaO, ZrO<sub>2</sub>, TiO<sub>2</sub> and Pr<sub>6</sub>O<sub>11</sub>. After ball-milling for 3 h, the mixture of raw materials was calcined at 600°C for two hours. The obtained powders were re-milled for one hour. The fine powder pressed into pellets (12 mm in diameter and 6 mm in thickness) by uniaxial pressing (ca. 70 MPa) using polyethylene glycol as binder. The pellets were sintered in the temperature range from 800 to 1000°C for 1/2 hour in air to get dense samples. Sintered pellets were polished for physical, microstructure and dielectric properties measurements. The density of the samples was measured by the Archimedes method with water as the liquid medium. The microstructure of samples were characterized by X-ray diffraction (XRD), (Rigaku D/max-A X-ray diffractometer) using CuKα radiation. Microstructures of fracture surfaces were observed by a scanning electron microscope (SEM) equipped with an energy-dispersive spectrometer (EDS). Dielectric properties as a function of frequency and temperature of the sintered disks was measured using an automatic measurement system with an A PM 6304 programmable automatic LCR bridge.

### III. RESULTS AND DISCUSSION

Figure 1 shows the water absorption% as a function of firing temperature. All investigated mixes showed a decrease in water absorption as temperature of firing increases. Physical properties results showed that, better densification is observed in discs fired at 1000 °C for 1/2 h, after that deformation started. All mixes showed low values of water absorption. Based on these results, 1000°C temperature was chosen the suitable maturing temperature.

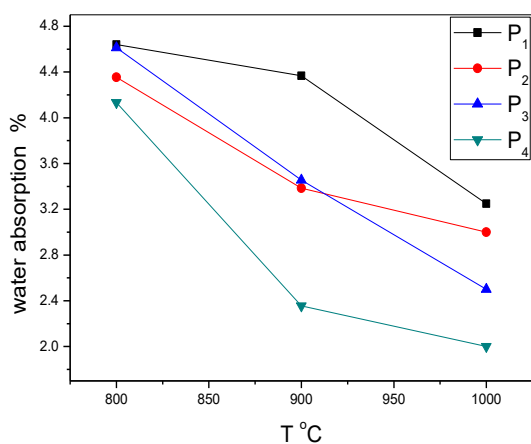


**Fig. 1** Water absorption % of the prepared samples as a function of firing temperature

The density of BaZrTiPrO<sub>8</sub> ceramic samples doped with various amounts of Pr<sub>6</sub>O<sub>11</sub> is shown in Fig.2. It is also clear that, as firing temperature increases the density of the prepared samples increases. Maximum density was realized at temperature of 1000 °C, and above 1000 °C sintering temperature, the density of all examined samples decreased. This decrease can be attributed to

the increase in intergranular porosity as a result of discontinuous grain growth [20, 21].

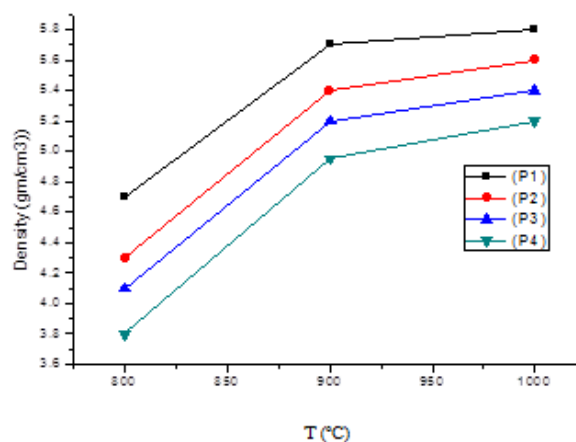


**Fig.2** Influence of sintering temperature on the density of the prepared samples.

Figure 3 indicate the compositional dependence of the water absorption and shrinkage % at temperature of 1000°C. Better densification of BaTiO<sub>3</sub> ceramics can be obtained by adding Pr<sub>6</sub>O<sub>11</sub> in current ZrO<sub>2</sub>. This is because the presence of closed pores was minimized. Sample (P<sub>4</sub>) of x = 0.6 mol% which fired at temperature of 1000 °C for 1/2 h recorded the minimum water absorption and maximum shrinkage %. Test results clearly indicated that minimum water absorption and improved densifications are realized in all samples subjected to fired temperature of 1000 °C for 1/ 2 h.

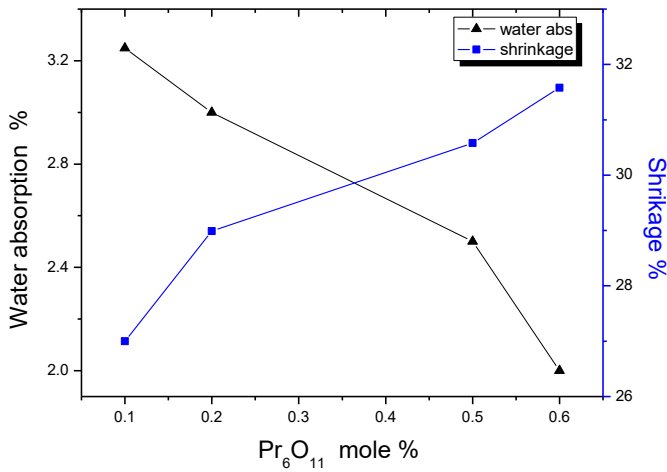


**Fig. 3** Compositional dependence of the water absorption % and shrinkage % of the prepared samples.

Figure 4 shows the x-ray diffraction patterns of the prepared samples. All compositions possess pure structure without any secondary phase to complete dissolution of the present dopants oxides in the lattice which form solid solution.

The average crystallite size ( $D$ ) BaZrTiO<sub>5</sub> ceramics has been calculated from x-ray data using Scherrer's equation [22, 23] and was found to increase with increasing Pr<sub>6</sub>O<sub>11</sub> content. The larger crystallite size may be due to the bridging of fine particles that formed the continuous grain boundary networks [24]. The maximum size of crystal was appeared in sample P<sub>3</sub> as illustrated in Fig.5. Further increase of Pr<sub>6</sub>O<sub>11</sub> causes a decrease in the crystalline size of the sample P<sub>4</sub> this may be attributed to the presence of some secondary phases of Pr<sub>2</sub>O<sub>3</sub> at the grain boundaries which delays the growth of grains

and creates an external pressure on the grains [25].

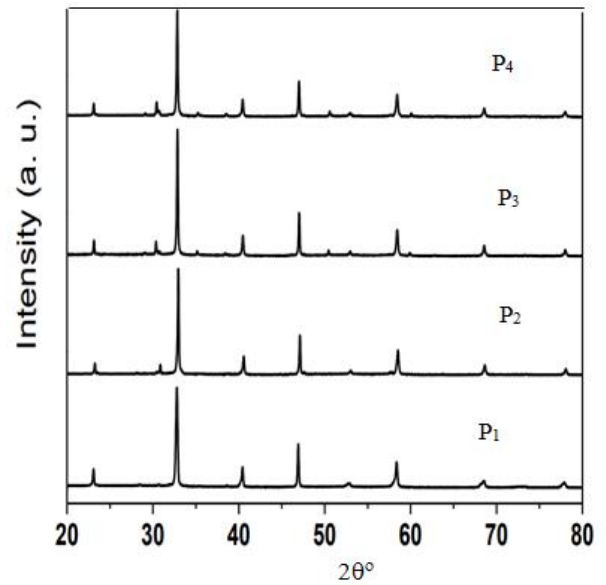


**Fig. 4** XRD of the prepared samples.

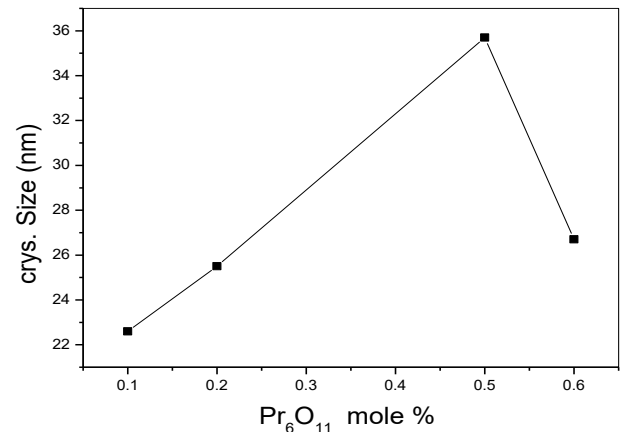


**Fig. 5** Variation of the crystallite size with Pr<sub>6</sub>O<sub>11</sub> mol %

The effect of increasing temperature on endothermic, weight loss and exothermic reaction were examined by the aid of TGA thermograms method for all the prepared samples, Fig. 6. A marginal weight loss of about 1% was observed in the TGA curve in the range between 100 and 300°C. This is attributed to the liberation of adsorbed moisture found in the sample as a result of the ultra-fine nature of the as prepared sample.

Strong endothermic was also revealed around at this temperature. A wide exothermic peak was recorded in the temperature region between 300°C and 600°C. In this region, the third loss in weight was noticed by burning Pr-based material in TGA curve. The existence of small exothermic peak in TG pattern at 258 °C can be due to intermediate reaction steps among the precursor material which leads to the creation of compound at a phase where mass loss reaches a saturation level. Thus the best appropriate temperature for calcinations to prepare the samples by a solid- state technique looks to be about 560°C.

The SEM of the samples P<sub>1</sub> and P<sub>3</sub> are shown in figure 7. SEM images show BaO grains are tend together and presence of pores of various sizes indicating a kind of volatilization, also Zr, Ti and Pr go into solid solution in the BaO grains.

Figure 8 shows the relation between V and I for all investigated samples in the present work. Figure 8 confirm the non linear, non-Omic current field characteristics of the prepared samples. The I-V relation of the samples P<sub>1</sub>, P<sub>4</sub> is placed as an inset of Fig.8 to clarify the the non-Ohmic behaviour of the samples. It is clear that all investigated samples show nonlinear I-V characteristics.

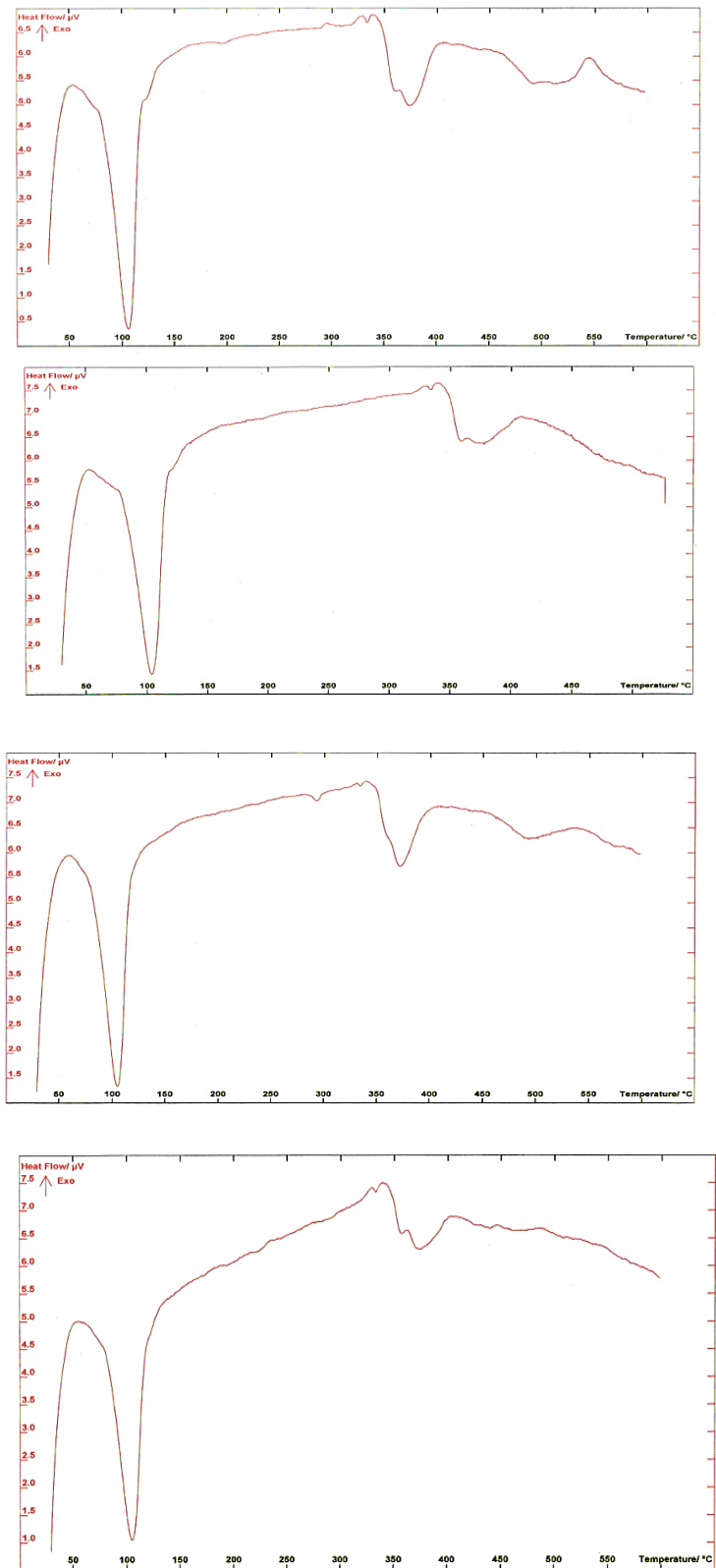
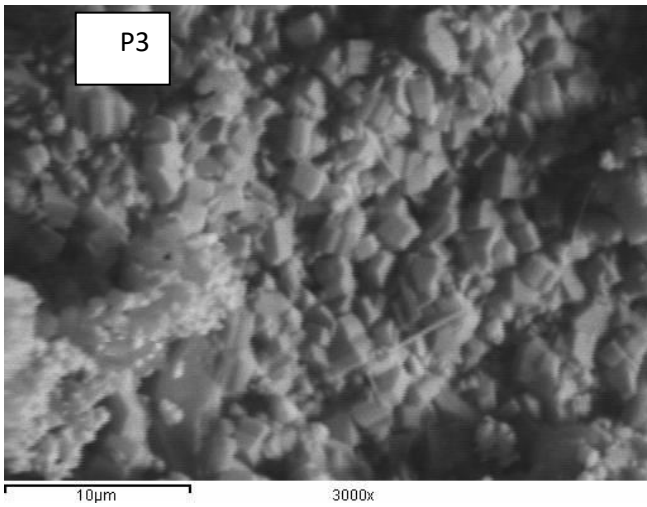
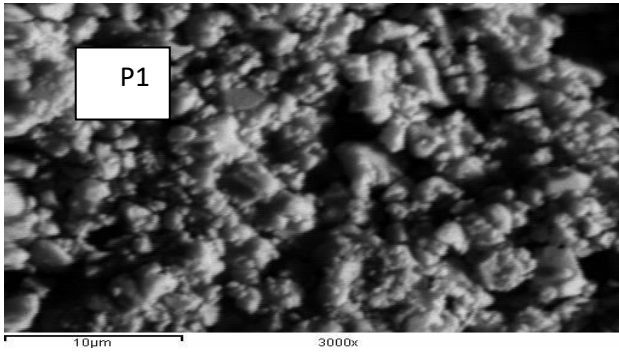


Fig. 6 TGA thermograms of all the prepared samples



**Fig.7** SEM images of the of the sample P<sub>1</sub> and P<sub>3</sub>

Also the breakdown field was measured as function of Pr<sub>6</sub>O<sub>11</sub> mol% and the obtained results are shown in figure 9. This figure shows that as Pr<sub>6</sub>O<sub>11</sub> mol% increases the breakdown field improved and attained its maximum value at 0.5mol % Pr<sub>6</sub>O<sub>11</sub> (Sample P<sub>3</sub>).The increase of the breakdoen field with increasig Pr<sub>6</sub>O<sub>11</sub> concentration is attributed to, the addition of small amount of Pr<sub>6</sub>O<sub>11</sub> may causes a thicker grain boundaries phase which reported elsewhere[26] which increases the effective barrier between the electrodes. Further addition of Pr<sub>6</sub>O<sub>11</sub> above 0.5 mol %

causes suppression of grain growth, as shown in Fig.5, and Pr<sub>6</sub>O<sub>11</sub> generates secondary phases at the grain boundaries and the valency state of praseodymium is changed into Pr<sub>2</sub>O<sub>3</sub> leading to change the donor concentration and decreasing the number of active barriers between the two electrodes and consequently the breakdown field decreases.[25].

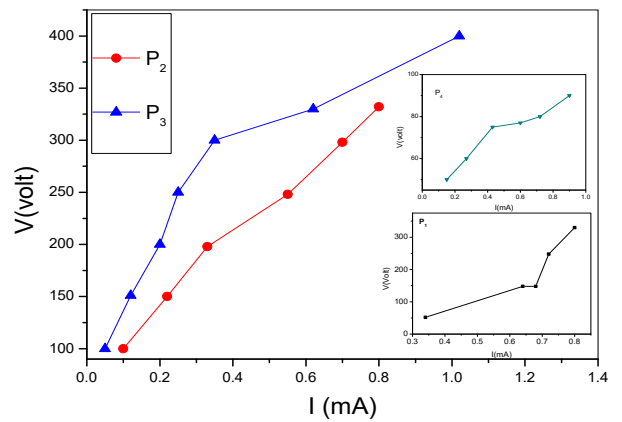


**Fig. 8.** (I -V) Characteristics of the prepared samples

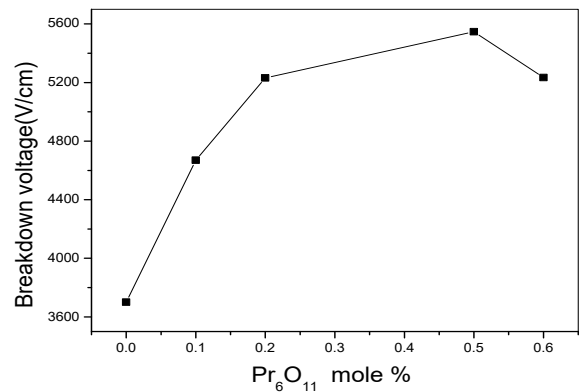


**Fig. 9** Breakdown field as a function of Pr<sub>6</sub>O<sub>11</sub> mole %

The dielectric constant of all the samples was measured as a function of frequency ranged from 1 to 20 kHz and the

obtained results are shown in Fig.10. It was found that, the dielectric constant ( $\epsilon'$ ) of all samples decreases with increasing frequency as shown in Fig.10. The sample P<sub>4</sub> which containing 0.6 mol% Pr<sub>6</sub>O<sub>11</sub> represents the maximum value of dielectric constant. As frequency increases the magnetic dipoles can not follow the variation of the electric field direction and consequently the dielectric constant decreases with the frequency.

The role played by praseodymium oxide in this case is during firing the valency state of praseodymium is changed into Pr<sub>2</sub>O<sub>3</sub> with the evolution of oxygen. The electronic interface states generation out grain boundaries is due to the evolution of such oxygen.

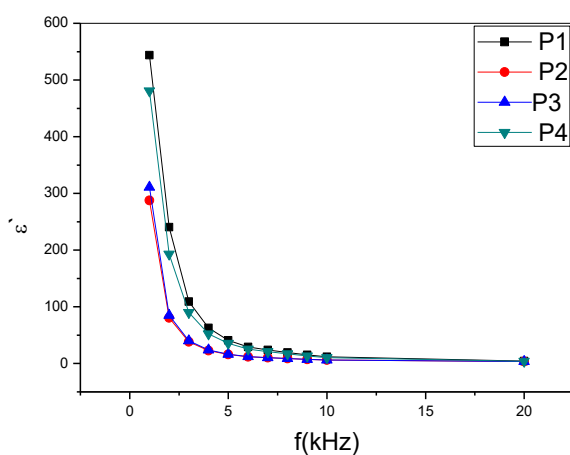
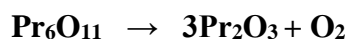


**Fig. 10** Variation of the dielectric constant with the frequency for all the prepared samples.

The relation between resistivity ( $\rho$ ) and frequency for all investigated mixes is

illustrated in Fig.11. The figure shows that as frequency increases the resistivity decreases. This is because increasing frequency of the applied field liberates the charges trapped in deep traps and increases the conductivity and consequently the resistivity decreases also the ionic response to the field at any certain frequency increases with increasing frequency.

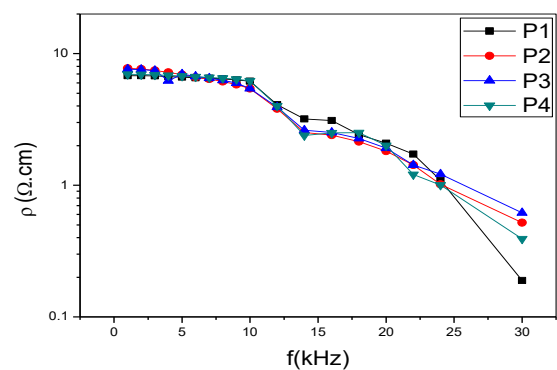


**Fig.11** Effect of the frequency on resistivity of the prepared samples

The compositional dependence of the dielectric constant and ac resistivity is shown in Fig. 12. The figure shows that, as Pr<sub>6</sub>O<sub>11</sub> content increases the ac resistivity increases and obtained its maximum value at 0.5 mol % of Pr<sub>6</sub>O<sub>11</sub> then decreases. The increase of the resistivity and decreases of the dielectric constant are due to the increase in the thickness of the poor conductive grain boundaries with increasing Pr<sub>6</sub>O<sub>11</sub> content. Also the increase in the ac resistivity is attributed to the increase of the average crystallite size which causes an increase in the intragranular porosity of the samples [27, 28]. Above 0.5 mol% the resistivity decreases because some of Pr<sub>6</sub>O<sub>11</sub> generate secondary phases of Pr<sub>2</sub>O<sub>3</sub> which

change the donor concentration at the grain boundaries [25]. The substitution of BaO by Pr<sub>6</sub>O<sub>11</sub> improves the physical properties of BaTiZrO<sub>5</sub> ceramics by increasing their breakdown field and ac resistivity makes these ceramics useful in the technological applications.

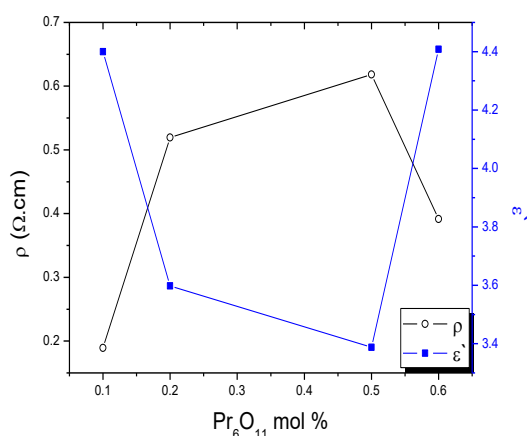


**Fig.12** Compositional dependence of the dielectric constant and ac resistivity of prepared samples

#### IV. CONCLUSIONS

1. BaZrTiPrO<sub>8</sub> ceramic samples have been successfully prepared by (conventional ceramic method) solid state reaction and their structure; physical and dielectric, properties have been studied.
2. Addition of Pr<sub>6</sub>O<sub>11</sub> in the presence of TiO<sub>2</sub>, ZrO<sub>2</sub> and BaO minimized the presence of closed pores and thus led to improved densification.
3. Samples exposed to fired temperature of 1000°C for 0.5 hour recorded the minimum water absorption and the maximum shrinkage.
4. Addition of Pr<sub>6</sub>O<sub>11</sub> improved breakdown field a further addition above 0.5 mol% is negatively affected.
5. It was found that, the substitution of BaO by Pr<sub>6</sub>O<sub>11</sub> improves the physical properties of

BaTiZrO<sub>5</sub> ceramics by increasing their breakdown field and ac resistivity while the dielectric constant decreases. The sample of 0.5 mol % has the highest breakdown field and ac resistivity makes these ceramics useful in the technological applications.

#### REFERENCES

- [1] C. Han, J. Wu, C. Pu, S. Qiao, B. Wu, J. Zhu, D. Xiao, "High piezoelectric coefficient of (Pr<sub>2</sub>Ca<sub>0.01</sub>)(Zr<sub>0.02</sub>Ti<sub>0.98</sub>)O<sub>3</sub>-doped Ba<sub>0.85</sub>Ca<sub>0.15</sub>Ti<sub>0.90</sub>Zr<sub>0.10</sub>O<sub>3</sub> ceramics", *Ceram Int.*, Vol. 38, pp 6359-6363, 2012.
- [2] P. Gao, L. J. Meng, M. P. Dos Santos, V. Teixeira, Andritschky "Study of ZrO<sub>2</sub>-Y<sub>2</sub>O<sub>3</sub> films prepared by rf magnetron reactive sputtering", *Thin Solid Films*, Vol. 377, pp 32-35, 2000.
- [3] A. Rae, M. Chu, V. Ganine, "Barium Titanate past, present and future", *Ceramic Transactions*, 100, pp 1-12, 1999.
- [4] T. Li, L.T. Li, Y. Kou, Z.L. Gui "Stable temperature dependence of dielectric properties in BaTiO<sub>3</sub>-Nb<sub>2</sub>O<sub>5</sub>-Co<sub>3</sub>O<sub>4</sub>-Gd<sub>2</sub>O<sub>3</sub> system", *J. Mater. Sci. Lett.*, Vol. 19, pp 995-997, 2000.
- [5] Emad K. Al-Shakarchi "Dielectric Properties of a BaTiO<sub>3</sub> Ceramic Prepared by Using the Freeze Drying Method", *J. Kore. Phys. Soc.*, Vol. 57, pp 245-250, 2010.
- [6] S. M. Neirman, "The Curie Point temperature of Ba (Ti<sub>1-x</sub>Zr<sub>x</sub>)O<sub>3</sub> Solid Solution", *J. Mater. Sci.*, Vol. 23, pp 3973-3980, 1988.
- [7] D. Hennings, Schnell, "A Diffuse Ferroelectric Phase Transitions in Ba(Ti<sub>1-y</sub>Zr<sub>y</sub>)O<sub>3</sub> Ceramics", *J. Am. Cer. Soc.*, Vol. 65, pp 539-534, 1982.
- [8] Weber, U. Greuel, G. Boettger, U. Weber, S. Hennings, D. ASER.R, "Dielectric Properties of Ba(Zr,Ti)O<sub>3</sub>-Based



- Ferroelectrics for Capacitor Applications”, J. Am. Ceram. Soc, Vol. 84, pp 759–66, 2001.
- [9] Rehrig, P. W. Park, S. E. McKinstry, S. T. Messing, G. L. Jones, et. al., “Piezoelectric properties of zirconium-doped barium titanate single crystals grown by templated grain growth”, J. Appl. Phys, Vol. 86, pp1657-1651, 1999.
- [10] E. Barringer, H. Kent Bowen “Formation, Packing, and Sintering of Monodisperse TiO<sub>2</sub> Powders”, J. Am. Ceram.Soc , 65, pp539, 1982.
- [11] D.F.K. Hennings, H. Schreinemacher, “Ca-acceptors in dielectric ceramics sintered in reductive atmospheres”, J. Eur. Ceram. Soc., Vol. 15, pp795–800, 1995.
- [12] H. Kishi, Y. Mizuno, H. Chazono, “Base-Metal Electrode-Multilayer Ceramic Capacitors: Past, Present and Future Perspectives”, Jpn. J. Appl. Phys, Vol. 42, pp1–15, 2003.
- [13] T.A. Jain, K.Z. Fung, J. Chan. “Effect of the A/B ratio on the microstructures and electrical properties of (Ba<sub>0.95±x</sub>Ca<sub>0.05</sub>) (Ti<sub>0.82</sub>Zr<sub>0.18</sub>)O<sub>3</sub> for multilayer ceramic capacitors with nickel electrodes”. J. Alloys Compd., Vol. 468, pp 370–374, 2009.
- [14] D. Hennings, H. Schreinemacher, “Temperature dependence of the segregation of calcium titanate from solid solutions of (Ba, Ca) (Ti, Zr)O<sub>3</sub> and its effect on the dielectric properties” Mat. Res. Bull., Vol. 12, pp 1221-1226, 1977.
- [15] G. A. Smolenskii, “Physical phenomena in ferroelectrics with diffused phase transition”, J. Phys. Soc. Jpn., Vol. 28, pp 26, 1970.
- [16] W. Chen, B. Liu, Q.F. Liu, S.T. Chen." “New mix design method for hpc-overall calculation method”. J Chin Ceram Soc., Vol. 28, pp194–8, 2000.
- [17] F. A. Ismail, R. A. Maulat Osman, M. S. Idris. “Review on dielectric properties of rare earth doped barium titanate”, AIP Conference Proceedings, Vol. 1756, pp 090005, 2016.
- [18] F.A. Ismail1, R.A. Maulat Osman, M.S. Idris and N.A.M. Ahmad Hambali, “Structure and electrical characteristics of BaTiO<sub>3</sub> and Ba<sub>0.99</sub>Er<sub>0.01</sub>TiO<sub>3</sub>”, Ceram. Solid State Phen., Vol. 280, pp127-133, 2018.
- [19] J. P. H. Lara, M. P. Labra, F. R. B. Hernández, J. A. R. Serrano, E. O. Á. Dávila, P. Thangarasu, A. H. Ramirez, “Structural evolution and electrical properties of BaTiO<sub>3</sub> doped with Gd<sup>3+</sup>”, Mater. Res., Vol. 20, pp 538-542, 2017.
- [20] Osama A Desouky, K E Rady. “Improvement of sintering, nonlinear electrical, and dielectric properties of ZnO-based varistors doped with TiO<sub>2</sub>” Chin. Phys. B., Vol. 25, 068402, 2016.
- [21] K.E. Rady and Osama A. Desouky. “Study of the effect of substitution by MnO<sub>2</sub> and V<sub>2</sub>O<sub>5</sub> on the microstructure, electrical and dielectric characteristics of zinc oxide ceramics”. Eur. Phys. J. Plus., Vol. 131, pp 444, 2016.
- [22] Osama A. Desouky, K. E. Rady. “Synthesis, structure and dielectric properties of nanocrystalline SnO<sub>2</sub>–CoO–Nb<sub>2</sub>O<sub>5</sub> varistor doped with Cr<sub>2</sub>O<sub>3</sub>”, J Mater Sci: Mater. Electron., Vol. 28, pp 4197-4203, 2017.
- [23] M.A. Ahmed , K.E. Rady, M.S. Shams. “Enhancement of electric and magnetic properties of Mn–Zn ferrite by Ni–Ti ions substitution”. J. All. Comp., Vol. 622, pp 269–275, 2015.
- [24] Hassanzadeh Tabrizi, S.A. Mazaheri, M. Aminzare, M. Sadrnezhaad, “Reverse precipitation synthesis and characterization of CeO<sub>2</sub> nanopowder”, J. All. Comp., Vol. 491, pp 499-502, 2010.
- [25] M. A. Ramírez, J. F. Fernández, J. de Frutos, P. R. Bueno, E. Longo, J. A. Varela, “Microstructural and nonohmic properties of

ZnO Pr6O11 CoO polycrystalline system".  
Mater. Res., Vol. 13, pp 29-34, 2010.

[26] J. Fan, R. Freer "Varistor properties and microstructure of ZnO–BaO ceramics" J. Mater. Sci., Vol. 32, pp 415, 1997.

[27] W.D. Kigery, H.K. Bowen, D.R. Uhlmann, Introduction of ceramics, John Wiley & Sons, New York, 1975.

[28] B. Rajesh Babu, K. V. Ramesh, M. S. R. Prasad, Y. Purushotham, "Structural, magnetic and dielectric properties of Ni<sub>0.5</sub>Zn<sub>0.5</sub>Al<sub>x</sub>Fe<sub>2-x</sub>O<sub>4</sub> nanoferrites" J. Supercon. Nov. Magn., Vol. 29, pp 939-950, 2016.